Microfluidic Formation of Hydrogel Microcapsules with a Single Aqueous Core by Spontaneous Cross-linking in Aqueous Two-Phase System (ATPS) Droplets

Takaichi Watanabe, Ibuki Motohiro, and Tsutomu Ono*

Division of Applied Chemistry, Graduate School of Natural Science, Okayama University, 3-1-1, Tsushima-naka, Kita-ku, Okayama, 700-8530, JAPAN

* Email: tono@okayama-u.ac.jp

Keywords: Emulsion, Poly(ethylene glycol), Phase separation, Core-shell, Janus, Encapsulation, Semi-permeable

Abstract

We report a simple process to fabricate monodisperse tetra-arm poly(ethylene glycol) (tetra-PEG) hydrogel microcapsules with an aqueous core and a semi-permeable hydrogel shell through the formation of aqueous two-phase system (ATPS) droplets consisting of dextran (DEX)-rich core and tetra-PEG macromonomer-rich shell, followed by spontaneous cross-end coupling reaction of tetra-PEG macromonomers in the shell. Different from conventional techniques, this process enables for the continuous production of hydrogel microcapsules from water-in-oil emulsion droplets under mild conditions in the absence of radical initiators and external stimuli such as heating and ultraviolet (UV) light irradiation. We find that rapid cross-end coupling reaction of tetra-

PEG macromonomers in ATPS droplets in the range of pH from 7.4 to 7.8 gives hydrogel microcapsules with a kinetically arrested core-shell structure. The diameter and core-shell ratio of the microcapsules can be easily controlled by adjusting flow rates and ATPS compositions. On the other hand, slow cross-end coupling reaction of tetra-PEG macromonomers in ATPS droplets at pH 7.0 and lower induces structural change from core-shell to Janus during the reaction, which eventually forms hydrogel microparticles with a thermodynamically stable crescent structure. We believe that these hydrogel microparticles with controlled structures can be used in biomedical fields such as cell encapsulation, biosensors, and drug delivery carriers for sensitive biomolecules.

Introduction

Microcapsules having a large aqueous core are attractive vehicles for the delivery of pharmaceuticals [1] and biologically active species [2-4], as well as for cell encapsulation [5-12]. Various techniques, including interfacial reaction [13], a co-extrusion [7,14,15], solvent evaporation from double emulsions [16-21], and deposition of polyelectrolyte layers on a sacrificial particle [22,23] are used to fabricate microcapsules. In particular, the most common way for the preparation of hydrogel microcapsules having an aqueous core and a semi-permeable hydrogel shell is to employ a co-extrusion of core-shell

droplets in air followed by a sol-gel transition of the shell after immersion of them into a gelling bath. However, this technique may lead to the formation of deformed microcapsules due to a rapid sol-gel transition at air-water interface [15].

Alternative strategy for the formation of microcapsules is to use double emulsion droplets as a template and solidify the shell by polymerization or solvent evaporation. Recent advancement in droplet-microfluidic techniques enables the formation of double emulsion droplets having various sizes, with low polydispersity by one-step, yielding monodisperse microcapsules with precisely controlled diameter and shell thickness [24-34]. However, the generation of monodisperse double emulsion droplets requires precise manipulation of multi-phasic flow to adjust the period of droplet breakup. Moreover, cross-linking reaction after droplet formation can be achieved by ultraviolet (UV) light irradiation or heating in the presence of radical initiators, which may lead to detrimental effect on encapsulated sensitive biomolecules and cells. Thus, it is desirable to develop an environmentally-friendly process to fabricate hydrogel microcapsules.

In this study, we propose a simple microfluidic approach to prepare monodisperse hydrogel microcapsules having an aqueous core and a hydrogel shell using aqueous two-phase system (ATPS) formation in monodisperse aqueous droplets, followed by spontaneous cross-linking reaction of macromonomer in the ATPS droplets, as shown in

Figure 1. In this process, microfluidic emulsification generates monodisperse aqueous droplets consisting of dextran (DEX) and two kinds of tetra-arm poly(ethylene glycol) (tetra-PEG) macromonomers, which phase separates to form ATPS droplets with a DEX-rich core and a tetra-PEG macromonomer-rich shell. Subsequently, spontaneous cross-linking of tetra-PEG macromonomers in the shell of the ATPS droplets occurs *via* cross-end coupling reaction, which yields monodisperse hydrogel microcapsules having a single aqueous core and a tetra-PEG hydrogel shell. Different from conventional techniques to fabricate hydrogel microcapsules, our approach is simple, rapid and environmentally-friendly because it does not require complex droplet templates and cross-linking stimuli such as UV light and heat. In addition, the shell of hydrogel microcapsules consists of tetra-PEG hydrogel that is well-known as a tough hydrogel [35-37], which would impart elastic modulus in MPa range to the resulting microcapsules. We demonstrate the continuous fabrication of tetra-PEG hydrogel microcapsules using a microfluidic system consisting of a cross-junction unit and an emulsification unit and investigate the effect of flow rates and ATPS compositions on the diameter and core-shell ratio of the microcapsules. We show that the shell of the microcapsules has selective permeability to molecules with different molecular weights, which can be applied to biomedical fields including drug delivery systems, bioreactors and regenerative

4

medicines. Finally, we also show that the structure of hydrogel microparticles can be controlled by tuning the reaction rate of tetra-PEG macromonomer in ATPS droplets.

Experimental Section

Material

All reagents were used as received. Pentaerythritol tetra(succinimidyloxyglutaryl) polyoxyethylene (TN-PEG, M_n = 10 kDa) and pentaerythritol tetra(aminopropyl) polyoxyethylene (TA-PEG, M_n = 10 kDa) were purchased from NOF Corporation, Japan. Dextran (DEX, M_w = 32 – 45 kDa), Span 80, tridecane, hexane, and toluene were purchased from FUJIFILM Wako Pure Chemical Corporation, Japan. Solsperse 19000 was kindly gifted from Lubrizol Corporation, Japan. Dextran labeled with fluorescein isothiocyanate (FITC-DEX, M_w = 250 kDa and 500 kDa) and trimethoxy(octadecyl)silane were purchased from Sigma-Aldrich, Japan. Reactive Blue 160 was purchased from MP Biomedicals, LLC. Deionized water with a resistance of 3 MΩ·cm was obtained by passing through Elix UV system.

Methods

Fabrication of a microfluidic device

We fabricated a glass capillary microfluidic device to prepare water-in-oil (W/O) emulsions, according to a previous report with minor modifications [24]. Briefly, a cylindrical glass capillary with inner and outer diameters of 0.6 mm and 1.0 mm, respectively (Narishige; G-1, Japan) was heated and pulled to achieve a tapered tip geometry by a pipette puller (Narishige; PC-10, Japan). The tips of two capillaries were polished using a sand paper (Sankyo Rikagaku Co., Ltd; #800, Japan) until their inner diameters reached about 120 μm (for injection capillary) and 270 μm (for collection capillary). To render the surfaces of the capillaries hydrophobic, they were treated with toluene solution containing 1 wt% of trimethoxy(octadecyl)silane at 110°C overnight prior to use. The two capillaries were coaxially localized in a square glass capillary with an inner diameter of 1.0 mm (VitroCom; Cat. No. 8100, USA). The distance between them was fixed about 100 μm. An epoxy glue (Nichiban Araldite, Japan) was used to fix the capillaries on a slide glass. A tube connector (for 1/16-inch, Index Health & Science, USA) was connected to a gap between two square glass capillaries using an epoxy glue. A cross-junction unit with inter diameter of 1.5 mm (ISIS Co., Ltd; VFX106, Japan) was attached to the inlet of injection capillary for dispersed phase using an epoxy glue. The distance between the cross-junction and the tip of injection capillary (emulsification point) was fixed at 1.5 cm. All inlets of the microfluidic device were connected to plastic

disposable syringes (Henke Sass Wolf, Germany) with PTFE tubes (for 1/16-inch, GL Science, Japan). The outlet of the collection capillary was connected to a sampling vial through PTFE tube (for 1/16-inch, GL Science, Japan). The syringes were set to syringe pumps (Harvard Apparatus 33, USA) to precisely control flow rates. The microfluidic device was placed on a stage of a digital microscope (VW-9000C, Keyence, Japan) with a high-speed camera (VW-600C, Keyence, Japan).

Phase mapping between tetra-PEG macromonomer and dextran

TA-PEG was dissolved in phosphate buffered saline (PBS, pH = 7.4) in the range of concentration from 12 to 56 %(w/w) and DEX was dissolved in PBS (pH = 7.4) in the range of concentration from 5.6 to 48 %(w/w). These aqueous solutions were mixed, and the total weight of the mixed solution was measured. Then, PBS was added into the mixed aqueous solution using a micropipette until the solution was changed from two phases to one phase. After the formation of one phase solution, the total weight of the solution was measured to calculate the final concentrations of TA-PEG and DEX. The experiment was conducted at 25°C.

Interfacial tension measurement

The interfacial tensions between 60 mg/mL TA-PEG in PBS (pH = 7.4) aqueous solution

and oil phase containing span80 or Solsperse 19000 and between 120 mg/mL DEX in

PBS (pH = 7.4) aqueous solution and oil phase containing span80 or Solsperse 19000

were measured with a Wilhelmy plate interfacial tension meter (K100, Kruss, Germany).

The interfacial tension was measured until it plateaued (~3600 sec). The experiment was

conducted at a constant temperature of 20°C.

Static contact angle measurement

The static contact angles were recorded with a DMo-501 (Kyowa Interface Science Co.,

Ltd.) drop shape analysis system equipped with a video camera. We prepared a tetra-PEG

hydrogel by mixing 60 mg of TA-PEG and 60 mg of TN-PEG in 1 mL of PBS (pH 7.4)

aqueous solution, pouring it in a petri dish, and leaving it to stand for 1 hour. Then, a 2.0

µL droplet of water or diiodomethane was placed on the surface of the tetra-PEG hydrogel

using a micropipette to measure the static contact angle (**Figure S2** and **Table S1**). The

surface free energy and parameters of these liquids are listed in **Table S2**. We also

measured the contact angles of a droplet of 120 mg/mL DEX aqueous solution and a

tridecane droplet containing 3 wt% Solsperse 19000 on the surface of tetra-PEG hydrogel

in the same manner (**Table S4**).

Preparation of polydisperse ATPS droplets containing DEX and tetra-PEG macromonomer by mechanical stirring

The preparation of ATPS droplets was based on W/O emulsion formation using mechanical stirring, followed by phase separation within each droplet. PBS solution (pH = 7.4) containing TA-PEG (60 mg/mL) and DEX (120 mg/mL) was prepared as a dispersed aqueous phase. The dispersed phase was subsequently emulsified with a tridecane solution containing 3 wt% Solsperse 19000 using a vortex mixer (Vortex-Genie2, Scientific Industries, USA) for 2 min. The resulting W/O emulsion droplets were observed with an optical microscope (BX51, Olympus, Japan).

Fabrication of monodisperse ATPS droplets using microfluidics

Monodisperse ATPS droplets were prepared by the generation of W/O emulsion droplets using microfluidics, followed by internal phase separation in each droplet. We prepared 90 mg/mL of TA-PEG in PBS aqueous solution (pH = 7.4) and 360 mg/mL of DEX in PBS aqueous solution (pH = 7.4) as a dispersed phase. Tridecane solution containing 3 wt% of Solsperse 19000 was prepared as a continuous phase. The DEX solution was fed into the central channel of the cross-junction and the TA-PEG solution was infused from

9

the both sides of the cross-junction. At the cross-junction (inner diameter = 1.5 mm), three

laminar streams consisting of DEX central stream and TA-PEG side streams were formed,

which were subsequently emulsified with the tridecane solution in a coaxial microfluidic

device, generating W/O emulsion droplets. When the droplets traveled to the downstream,

phase separation spontaneously occurred between TA-PEG-rich phase and DEX-rich

phase, leading to the formation of water-in-water-in-oil (W/W/O) emulsion droplets.

Fabrication of tetra-PEG hydrogel microcapsules using microfluidics

We prepared 90 mg/mL of TA-PEG in PBS aqueous solution (pH = 7.4), 90 mg/mL of

TN-PEG in PBS aqueous solution (pH = 7.4), and 360 mg/mL of DEX in PBS aqueous

solution (pH = 7.4) as a dispersed phase. A tridecane solution containing 3 wt% of

Solsperse 19000 was prepared as a continuous phase. The DEX solution was fed into the

central channel of the cross-junction, whereas both TN-PEG and TA-PEG solutions were

infused from each side of the cross-junction. At the cross-junction (inner diameter = 1.5

mm), three laminar streams consisting of DEX central stream and TN-PEG and TA-PEG

side streams were formed, which were subsequently emulsified with the tridecane

solution in a coaxial microfluidic device, generating W/O emulsion droplets. When the

droplets traveled to the downstream, phase separation occurred in each droplet, which

lead to the formation of W/W/O emulsion droplets consisting of a DEX-rich core and a

tetra-PEG macromonomer-rich shell. Subsequently, the tetra-PEG macromonomer-rich

shell spontaneously began gelation *via* cross-end coupling reaction between TN-PEG and

TA-PEG, which resulted in the formation of hydrogel microcapsules. The resulting

hydrogel microcapsules were collected in a sampling bottle filled with a tridecane

solution containing 3 wt% of Solsperse 19000. The hydrogel microcapsules were then

washed with hexane and deionized water to remove remaining surfactant, tetra-PEG

macromonomers, and DEX. The resulting hydrogel microcapsules were observed with an

optical microscope (BX51, Olympus, Japan). To evaluate the effect of pH on the resultant

structure of hydrogel particles, we also performed the preparation of hydrogel

microparticles using the microfluidic technology at different pH conditions of aqueous

dispersed phase. The pH was changed in the range between 4.0 and 8.2.

Permeability measurement of hydrogel microcapsules

Hydrogel microcapsules were suspended in PBS solution containing 0.1 wt% FITC-DEX

with different molecular weights. The diffusion of FITC-DEX inside the hydrogel

microcapsules was imaged at 0 h and 24 h after the onset of experiment by a confocal

microscope (FV1000, Olympus, Japan) using an excitation light at 490 nm and an

emission light at 520 nm.

Results and Discussion

Phase Diagram Between Tetra-PEG Macromonomer and DEX

ATPS systems between PEG and DEX aqueous solutions have been considerably

studied and applied to various applications such as protein separation [38,39], cell

partitioning [40], templates for microcapsules [41-44], and encapsulation of cells and

bacteria [45,46]. In this study, ATPS droplets consisting of a DEX core and a tetra-PEG

macromonomer shell are employed as a template for hydrogel microcapsules. To

determine ATPS compositions, we first constructed a phase diagram between tetra-PEG

macromonomer and DEX aqueous solutions, which gives required pairs of polymer

concentrations to form ATPS. Here we assumed that tetra-PEG macromonomers with

different termini (ex. TA-PEG and TN-PEG) have the same interaction with DEX because

they have the same polymer backbone. Then, we selected TA-PEG as a representative

tetra-PEG macromonomer to construct the phase diagram.

Figure 2 shows a phase diagram between TA-PEG and DEX aqueous solutions.

The dashed line in Fig. 2 is a binodal curve indicating critical concentrations of polymers

above which two-phase system forms, whereas concentrations below the binodal curve

gives a single aqueous phase. Based on this result, we determined to use ATPS consisting

of 60 mg/mL tetra-PEG macromonomer and 120 mg/mL DEX as a standard composition

for ATPS droplet formation, plotted with an open square symbol in Fig. 2, because this

composition near the binodal curve provides a dispersed aqueous phase with relatively

low viscosity that is favorable for droplet-breakup in microfluidics.

Formation of ATPS Droplets with a Core-Shell Structure

To prepare hydrogel microcapsules having an aqueous core and a tetra-PEG

hydrogel shell, precursor ATPS droplets should be a core-shell structure. Based on the

spreading coefficient theory established by Torza and Mason [47], thermodynamically

stable structure of ATPS droplets can be predicted and controlled by the relative

magnitude of interfacial tensions among three phases including two kinds of aqueous

phases and an oil phase. As illustrated in **Figure 3a**, for phase-separated aqueous liquids

(tetra-PEG macromonomer-rich phase and DEX-rich phase) suspended in an oil, the

DEX-rich phase can be completely engulfed in the tetra-PEG macromonomer-rich phase

if the interfacial tension between the tetra-PEG macromonomer-rich phase and the oil

phase ($\gamma_{PEG-Oil}$) are lower than that between the DEX-rich phase and the oil phase

($\gamma_{DEX-Oil}$). Because interfacial tensions are significantly influenced by the types of oil

phase and surfactant, we determined the compositions of oil phase that can be suitable to

form core-shell structures in ATPS droplets by measuring interfacial tensions between various water-oil interfaces. The results of interfacial tension measurements are presented in **Table 1**. Regardless of the types of oil phases used in this study, $\gamma_{PEG-Oil}$ is smaller than $\gamma_{DEX-Oil}$ even in the case without surfactant, probably because DEX is more hydrophilic than PEG and PEG is more hydrophobic than DEX, even though PEG is a highly water-soluble polymer [48]. This result suggests that the predicted thermodynamically stable structure of the ATPS droplets is core-shell when using these oil phases.

To confirm the formation of aqueous droplets with a core-shell structure, we prepared aqueous droplets containing 60 mg/mL of tetra-PEG macromonomer (TA-PEG) and 120 mg/mL of DEX dispersed in a tridecane containing 3 wt% of Solsperse 19000 by means of mechanical emulsification and observed the structural change in aqueous droplets during ATPS formation. A homogeneous premix aqueous solution containing TA-PEG and DEX was emulsified with a continuous tridecane solution using a vortex mixer, generating single-phase aqueous droplets at the initial stage because the composition of TA-PEG and DEX in the aqueous phase is fixed near the binodal line and relatively longer time is needed to begin phase separation. After the formation of aqueous mixture droplets, phase separation occurred in the droplets, leading to the formation of

ATPS droplets having a core-shell structure. To understand the detailed structure of the

ATPS droplets, we also prepared ATPS droplets with a trace amount of Reactive Blue 160

to color tetra-PEG macromonomer-rich phase blue and observed the location of the tetra-

PEG macronomer-rich phase through optical microscopy observation (**Figure 3b**). The

color of the shell region of the droplets showed blue, implying that the resulting ATPS

droplets consist of a DEX-rich core and a tetra-PEG macromonomer-rich shell. These

results show that the thermodynamically stable structure of the ATPS droplets can be

predicted by the spreading coefficient theory and ATPS droplets with a DEX-rich core

and a tetra-PEG macromonomer-rich shell can be obtained by phase separation between

DEX and tetra-PEG macromonomer in aqueous droplets.

Flow Conditions to Generate Monodisperse ATPS Droplets

To produce monodisperse ATPS droplets as a template for hydrogel

microcapsules, we constructed a hybrid microfluidic system consisting of a cross-junction

unit and a coaxial emulsification unit. Then, we explored the effect of flow rate ratios

between dispersed phase (Q_d) and continuous phase (Q_c) on droplet formation by using a

model emulsion system in the absence of cross-end coupling reaction. For the model

emulsion system, we used an aqueous solution containing one kind of tetra-PEG

macromonomer (TA-PEG, 60 mg/mL) and DEX (120 mg/mL) as a dispersed phase and

a tridecane solution with 3 wt% Solsperse 19000 as a continuous phase. To form droplets

containing two kinds of dispersed aqueous solutions, we introduced these solutions into

a cross-junction unit as three laminar streams consisting of DEX solution as a central

stream and TA-PEG solution as side streams. Because we operated these solutions under

laminar flow conditions, mixing of the three laminar streams prior to droplet breakup was

suppressed. The laminar streams were then emulsified with the continuous oil phase at

the flow focusing point in the coaxial microfluidic device. Upon emulsification, the DEX

and TA-PEG in aqueous droplets were partially mixed; however, phase separation

proceeded in the droplets flowing toward the downstream of the channel, leading to the

formation of ATPS droplets.

It is well-known that droplet generation in microfluidics is affected by various

parameters including the flow rate of each phase, their viscosities, interfacial tensions,

and channel geometry [49]. There are two main mechanisms of droplet breakup in

microfluidics: dripping and jetting. These droplet breakup behaviors can be characterized

by the capillary number of the continuous phase, $C_a = \mu_c v_c / \gamma$, where μ_c, v_c, and γ

are the viscosity, velocity of the continuous phase, and interfacial tension, and the Weber

number of the dispersed phase, $W_e = \rho_d d_{tip} v_d{}^2 / \gamma$, where ρ_d, d_{tip}, and v_d are the

density of the dispersed phase, inner diameter of capillary tube, and velocity of the

dispersed phase. To investigate flow conditions that give monodisperse emulsion droplets,

we constructed a state diagram that shows approximate boundary between dripping and

jetting in the microfluidic device using two dimensionless numbers: C_a and W_e

(**Figure 4a**). We found that monodisperse droplets were formed in the dripping regime

(the values of C_a and W_e were in the range of 0.1 to 1.6 and 0.1 to 2.8), while unstable

droplet formation resulted in polydisperse droplets in the jetting regime.

To evaluate time scale of phase separation within aqueous droplets in the

dripping regime, we performed *in-situ* observation of the droplets in the microfluidic

device by using a digital microscope equipped with a high-speed camera. We found that

phase separation in the droplets proceeded as a function of time, which eventually lead to

the formation of a core-shell structure at 0.5 sec after droplet formation (**Figure 4b**). We

also found that the resultant ATPS droplets consisted of a DEX-rich core and a tetra-PEG

macromonomer-rich shell (**Figure 4c**).

The state diagram proposed in this study is based on the model emulsion system

without cross-end coupling reaction. However, we envision that this state diagram will

provide useful information for the fabrication of monodisperse hydrogel microcapsules

in our system, because the initial fluids parameters such as viscosities and interfacial

tensions correspond to those of the emulsion system used for the formation of hydrogel microcapsules in the following section.

Formation of Hydrogel Microcapsules with a DEX Core and a Tetra-PEG Hydrogel Shell

Next, we demonstrated the preparation of monodisperse hydrogel microcapsules using a reactive emulsion system consisting of an aqueous solution with two kinds of tetra-PEG macromonomers (TN-PEG and TA-PEG) and DEX as a dispersed phase and tridecane solution with Solsperse 19000 as a continuous phase using microfluidic technology. To prevent the microfluidic device from clogging by rapid cross-end coupling reaction between TN-PEG and TA-PEG when they are directly in contact with each other prior to emulsification, three kinds of aqueous phases including TA-PEG macromonomer, TN-PEG macromonomer, and DEX were separately injected into the microfluidic device from three inlets, which form three laminar streams consisting DEX central stream and TN-PEG and TA-PEG side streams. After emulsification, ATPS droplets having a DEX-rich core and a tetra-PEG macromonomer-rich shell were formed due to phase separation in the droplets. The migration of tetra-PEG macromonomers to the shell in the ATPS droplets increased the local concentration of tetra-PEG macromonomers and facilitated

18

gelation of the shell *via* their cross-end coupling reaction, which eventually formed hydrogel microcapsules with a DEX-core and a tetra-PEG hydrogel shell (**Figure 5a**).

To confirm the formation of hydrogel microcapsules, the hydrogel microcapsules collected in tridecane were re-suspended in water and observed with an optical microscope. **Figure 5b** shows the optical microscopy image of the hydrogel microcapsules suspended in water. When the microcapsules were transferred from oil to water phase, the microcapsules quickly swelled because of water uptake in the microcapsules, while keeping the core-shell structure intact. The diameter of microcapsules was increased from 206.5 μm ($CV = 5.3\%$) in oil phase to 305.9 μm ($CV = 9.1\%$) in water phase. These results clearly show that the microcapsules possess hydrogel properties undergoing swelling-deswelling transitions. Regarding a mechanical perspective of tetra-PEG hydrogel shell, the hydrogel microcapsules exhibited elasticity following compression. Even when sufficient pressure was exerted, the microcapsules deformed, but they quickly returned to the original core-shell structure after releasing the pressure (**Figure 5c**). On the other hand, all hydrogel microcapsules suspended in water had micron-sized pores in their shell, which indicates incomplete phase separation in ATPS droplets as described in other study [50].

The dimeter of microcapsules can be tuned by adjusting the flow rate ratios

between the dispersed and continuous phases. We prepared microcapsules by changing

the flow rate of the continuous phase, while keeping that of the dispersed phase constant

at 150 μL/min. As shown in **Figure 6a-c**, the diameter of the microcapsules decreased

with increasing the flow rate of continuous phase. The *CV* values of the microcapsules

were less than 10%, regardless of the flow conditions, showing that the microcapsules

have relatively narrow size distributions. Moreover, it was found that shell thickness to

radius (T/R) ratio was kept approximately constant regardless of the flow rates (**Table 2**).

We also demonstrated the control of the shell thickness in microcapsules by tuning the

flow rates of each dispersed aqueous phase, while keeping that of the continuous phase

at 800 μL/min (**Figure 6d-f**). The T/R ratio was increased with decreasing the

concentration ratio of DEX (C_{DEX}) to tetra-PEG macromonomers (C_{PEG}) in the dispersed

aqueous phase (**Table 3**). These results show that our process can readily control the

dimensions of hydrogel microcapsules just by tuning flow rates and ATPS compositions.

To investigate the molecular permeability of the shell of tetra-PEG hydrogel

microcapsules, we put hydrogel microcapsules in PBS solutions dissolving FITC-DEX

with different molecular weights (250 kDa and 500 kDa) and observed the diffusion

behavior of the FITC-DEX into the hydrogel microcapsules by confocal microscopy

observation (**Figure 7**). The 250 kDa FITC-DEX permeated into the hydrogel

microcapsules within 24 hours, as indicated by an increase in the fluorescent intensity in the core of hydrogel microcapsules. In contrast, the 500 kDa FITC-DEX exhibited less permeation into the hydrogel microcapsules even after 24 hours. These results suggest that our hydrogel microcapsules with semi-permeable membrane have a potential to be drug delivery carriers with molecular weight-dependent controlled release of encapsulated molecules and 3D culture of cells for regenerative medicines. If Stoke's diameter of 500 kDa FITC-DEX represents the mesh size of the hydrogel shell, the mesh size is thought to be in the range of 20 ~ 27.6 nm [51]. However, this mesh size is considerably larger than that of bulk tetra-PEG hydrogel (~ 10 nm) estimated from correlation length by small angle neutron scattering measurement [52]. This is because the shell of the hydrogel microcapsules contains small amount of DEX domains (non-cross-linked region) due to ATPS partitioning and incomplete phase separation. We consider that further study will be needed to control the mesh size of tetra-PEG hydrogel microcapsules by tuning molecular weight and concentration of tetra-PEG macromonomers.

To control the rate of cross-end coupling reaction, we varied pH value of the dispersed aqueous phase from 7.4 to 4.0 and prepared hydrogel microcapsules in the same manner. We expected that the rate of cross-end coupling reaction of tetra-PEG

macromonomer decreases when changing the pH from 7.4 to 4.0, and that lower pH gives

longer time to form hydrogel microparticles from W/W/O emulsion droplets. At both pH

conditions, we obtained ATPS droplets with a core-shell structure after phase separation.

However, surprisingly, in the case of pH at 4.0, the structural change in ATPS droplets

occurred as the cross-end coupling reaction proceeded, eventually leading to tetra-PEG

hydrogel microparticles with a Janus structure (**Figure 8**). This result indicates that

thermodynamically stable structure in this system changes before and after cross-end

coupling reaction, and that tetra-PEG hydrogel microcapsules with a core-shell structure

obtained at pH 7.4 is not a thermodynamically stable structure, but a kinetically-arrested

structure after cross-end coupling reaction. We found that interfacial tension between

tetra-PEG hydrogel and oil phase (after cross-end coupling reaction) was significantly

larger than that between tetra-PEG macromonomer-rich phase and oil phase (before

cross-end coupling reaction) and that predicted thermodynamically stable structure

altered from core-shell to acorn structure during cross-end coupling reaction (**Figure S3**).

Moreover, we found that when the Janus hydrogel particles were transferred from oil to

water phase, the DEX in the Janus particles was washed out, leading to crescent tetra-

PEG hydrogel microparticles (**Figure 9**). These results suggest that our process can be

used to prepare hydrogel microparticles with both thermodynamically stable and

kinetically arrested structures by tuning the rate of cross-end coupling reaction.

To evaluate what time scale of cross-end coupling reaction gives hydrogel capsules with a core-shell structure under kinetically arrested conditions in our system, we performed the preparation of tetra-PEG hydrogel particles in the range of pH between 6.0 and 8.2 and observed the resultant particle structures. When changing pH value from 6.0 to 8.2, gelation time (t_{gel}) of tetra-PEG hydrogel varied from 1,050 to 12 sec (**Figure 10a**). **Figure 10b-e** show the representative optical microscopy images of tetra-PEG hydrogel microparticles prepared at different pH conditions (pH = 7.0, 7.4, 7.8, and 8.0). We found that when the pH was 7.0 or lower (at $t_{gel} \geqq 270$ sec), hydrogel particles with a crescent structure were formed under thermodynamically stable structure (Fig. 10b). We also found that tetra-PEG hydrogel microcapsules with a core-shell structure were obtained at pH 7.8 and 7.4 under kinetically arrested conditions, which corresponded to the range of t_{gel} between 15 and 100 sec (Fig. 10c and d). When the pH was 8.0 or larger (at $t_{gel} < 13$ sec), we obtained hydrogel capsules with multi-core structures under kinetically arrested conditions, because the gelation was rapidly achieved before the formation of ATPS core-shell droplets (Fig. 10e). Based upon these results, we concluded that in our system, hydrogel capsules with a single aqueous core are formed under kinetically arrested conditions when t_{gel} is in the range of 15 and 100 sec after droplet

23

formation.

Conclusions

We have reported that the combination of ATPS droplet formation in microfluidics and subsequent spontaneous cross-end coupling reaction provides a simple route to the formation of hydrogel microcapsules with a single aqueous core. With the aid of a capillary microfluidic device, aqueous droplets containing DEX and tetra-PEG macromonomer are generated, which subsequently begin internal phase separation between DEX-rich core and tetra-PEG macromonomer-rich shell. The migration of tetra-PEG macromonomer to the shell of ATPS droplets facilitates spontaneous cross-end coupling reaction between tetra-PEG macromonomers, yielding microcapsules with a DEX core and a tetra-PEG hydrogel shell. The hydrogel microcapsules exhibit hydrogel properties such as swelling-deswelling behavior, elasticity upon exerting pressure on the microcapsules and semi-permeability of hydrogel shell. The diameter and core-shell ratio of the microcapsules can be easily controlled by adjusting the flow rates and ATPS compositions. Moreover, we find that tetra-PEG hydrogel microcapsules with a core-shell structure are kinetically arrested structure because of rapid cross-end coupling reaction at pH 7.4 in core-shell aqueous droplets, while slow cross-end coupling reaction at pH 4.0

in core-shell aqueous droplets gives crescent-shaped tetra-PEG hydrogel microparticles as thermodynamically stable structure. We also find that in our system, hydrogel microcapsules with a single aqueous core are formed when the time scale of gelation is between 15 and 100 sec after droplet formation. We believe that hydrogel microcapsules developed in our system would be promising candidates for cell encapsulation, biosensors, and drug delivery systems.

Associated Content

Supporting Information.

The Supporting Information is available free of charge on the ACS Publications Website at DOI:

Calculation of surface and interfacial free energy of tetra-PEG hydrogel; the Young equation using the interfacial free energy γ_{SL} at the solid and liquid (L) interfaces; the surface free energy can be divided into a disperse part (dispersion force (γ^d)) and a polar part (polar force (γ^p)) components; the Owens-Wendt equation; the spreading coefficient equations; definition of static contact angle (θ) of liquid on a solid surface in air;

photographs (side view) of water and diiodomethane droplets on tetra-PEG hydrogel in air; contact angle of water and diiodomethane droplets on the surface of tetra-PEG hydrogel; surface free energy of tetra-PEG hydrogel determined by Owens-Wendt method; Surface tensions of DEX aqueous solution and continuous oil phase measured by the Wilhelmy plate method; photographs (side view) of a 120 mg/mL of DEX aqueous droplet and a tridecane droplet containing 3 wt% Solsperse 19000 on the surface of tetra-PEG hydrogel in air; contact angle of a droplet of 120 mg/mL DEX aqueous solution and a tridecane droplet containing 3 wt% Solsperse 19000 on the surface of tetra-PEG hydrogel in air; interfacial tensions among three phases including tetra-PEG hydrogel, 120 mg/mL DEX aqueous solution and tridecane solution containing 3 wt% Solsperse 19000 (Oil phase); spreading coefficient of ATPS droplets before and after cross-end coupling reaction of tetra-PEG macromonomers; schematic images of possible structures of ATPS droplets after phase separation, predicted from spreading coefficient calculated using interfacial tensions

Author Information

Corresponding Author

*E-mail: tono@okayama-u.ac.jp

Tel: +81-86-251-8072; Fax: +81-86-251-8072.

Author Contributions

T.W., I. M., and T. O. designed the experiments. I. M. performed all the experiments and T. W. and I. M. analyzed the data. T. W., I. M., and T. O. interpreted the results. T. W. wrote the manuscript. T. W. and T. O. designed the research.

Notes

The authors declare no competing financial interest.

References

[1] Nan, F.; Wu, Jie.; Qi, F.; Ma, G.; Ngai, T. Preparation of uniform-sized colloidosomes based on chitosan-coated alginate particles and its application for oral insulin delivery. *J. Mater. Chem. B* **2014**, *2*, 7403-7409.

[2] Liu, W.; Wen, S.; Shen, M.; Shi, X. Doxorubicin-loaded poly(lactic-co-glycolic acid) hollow microcapsules for targeted drug delivery to cancer cells. *New J. Chem.* **2014**, *38*, 3917-3924.

[3] Pessi, J.; Santos, A. H.; Miroshnyk, I.; Yliruusi, J.; Weitz, D. A.; Mirza, S. Microfluidics-assisted engineering of polymeric microcapsules with high encapsulation efficiency for protein drug delivery. *Int. J. Pharm.* **2014**, *472*, 82-87.

[4] Donnell, P. B.; McGinity, J. W. Preparation of microspheres by the solvent evaporation technique. *Adv. Drug Deliv. Rev.* **1997**, *28*, 25-42.

[5] De Temmerman, M. L.; Demeester, J.; De Vos, F.; De Smedt, S. C. Encapsulation Performance of Layer-by-Layer Microcapsules for Proteins. *Biomacromolecules* **2011**, *12*, 1283-1289.

[6] Chang, T. M. Semipermeable Microcapsules. *Science*, **1964**, *146*, 524-525.

[7] Ma, M.; Chiu, A.; Sahav, G.; Doloff, J. C.; Dholakia, N.; Thakrar, R.; Cohen, J.; Vegas, A.; Chen, D.; Bratlie, K. M.; Dang, T.; York, R. L.; Hollister-Lock, J.; Weir, G. C.; Anderson, D. G. Core-Shell Hydrogel Microcapsules for Improved Islets Encapsulation. *Adv. Healthcare Mater.* **2013**, *2*, 667-672.

[8] Rossow, T.; Heyman, J. A.; Ehrlicher, A. J.; Langhoff, A.; Weitz, D. A.; Haag, R.; Seiffert, S. Controlled Synthesis of Cell-Laden Microgels by Radical-Free Gelation in Droplet Microfluidics. *J. Am. Chem. Soc.* **2012**, *134*, 4983-4989.

[9] Esfahani, R. R.; Jun, H.; Rahmani, S.; Miller, A.; Lahann, J. Microencapsulation of Live Cells in Synthetic Polymer Capsules. *ACS Omega* **2017**, *2*, 2839-2847.

[10] Hackelbusch, S.; Rossow, T.; Steinhilber, D.; Weitz, D. A.; Seiffert, S. Hybrid Microgels with Thermo-Tunable Elasticity for Controlled Cell Confinement. *Adv. Healthcare Mater.* **2015**, *4*, 1841-1848.

[11] Zhao, G.; Liu, X.; Zhu, K.; He, X. Hydrogel Encapsulation Facilitates Rapid-Cooling Cryopreservation of Stem Cell-Laden Core–Shell Microcapsules as Cell–Biomaterial Constructs. *Adv. Healthcare Mater.* **2017**, *6*, 1700988.

[12] Hann, S. D.; Niepa, T. H. R.; Stebe, K. J.; Lee, D. One-Step Generation of Cell-Encapsulating Compartments via Polyelectrolyte Complexation in an Aqueous Two Phase System. *ACS Appl. Mater. Interfaces* **2016**, *8*, 25603-25611.

[13] Zhang, J.; Coulston, R. J.; Jones, S. T.; Geng, J.; Scherman, O. A.; Abell, C. One-Step Fabrication of Supramolecular Microcapsules from Microfluidic Droplets. *Science* **2012**, *335*, 690-694.

[14] Nguyen, D. K.; Son, Y. M.; Lee, N. E. Hydrogel Encapsulation of Cells in Core-Shell Microcapsules for Cell Delivery. *Adv. Healthcare Mater.* 2015, **15**, 1537-1544.

[15] Domejean, H.; Saint Pierre, M. D.; Funfak, A.; Atrux-Taullau, N.; Alessandri, K.; Nassoy, P.; Bibette, J.; Bremond, N. Controlled production of sub-millimeter liquid core hydrogel capsules for parallelized 3D cell culture. *Lab Chip* **2017**, *17*, 110-119.

[16] Yan, C.; Resau, J. H.; Hewetson, J.; West, M.; Rill, W. L.; Kende, M. Characterization and morphological analysis of protein-loaded poly(lactide-co-glycolide) microparticles prepared by water-in-oil-in-water emulsion technique. *J. Controlled Release* **1994**, *32*, 231-241.

[17] Iqbal, M.; Zafar, N.; Fessi, H.; Elaissari, A. Double emulsion solvent evaporation techniques used for drug encapsulation. *Int. J. Pharm.* **2015**, *496*, 173-190.

[18] Hong, L.; Sun, G.; Cai, J.; Ngai, T. One-Step Formation of W/O/W Multiple Emulsions Stabilized by Single Amphiphilic Block Copolymers. *Langmuir* **2012**, *28*, 2332-2336.

[19] Kim, M. R.; Cheong, I. W. Stimuli-triggered Formation of Polymersomes from W/O/W Multiple Double Emulsion Droplets Containing Poly(styrene)-block-poly(N-isopropylacrylamide-co-spironaphthoxazine methacryloyl). *Langmuir* **2016**, *32*, 9223-9228.

[20] Watanabe, T.; Sakamoto, Y.; Inooka, T.; Kimura, Y.; Ono, T. Indocyanine green-laden poly(ethylene glycol)-block-polylactide (PEG-b-PLA) nanocapsules incorporating reverse micelles: Effects of PEG-b-PLA composition on the nanocapsule diameter and encapsulation efficiency. *Colloids Surf. A: Physicochem. Eng. Aspects* **2017**, *520*, 764-770.

[21] Yu, X.; Zhao, Z.; Nie, W.; Deng, R.; Liu, S.; Liang, R.; Zhu, J. Ji, X. Biodegradable Polymer Microcapsules Fabrication through a Template-Free Approach. *Langmuir* **2011**, *27*, 10265-10273.

[22] Tong, W.; Song, X.; Gao, C. Layer-by-layer assembly of microcapsules and their biomedical applications. *Chem. Soc. Rev.* **2012**, *41*, 6103-6124.

[23] Zhang, W.; Zhao, S.; Rao, W.; Snyder, J.; Choi, J. K.; Wang, J.; Khan, I. A.; Saleh, N. B.; Mohler, P. J.; Yu, J.; Hund, T. J.; Tang, C.; He, X. A novel core-shell microcapsule for encapsulation and 3D culture of embryonic stem cells. *J. Mater. Chem. B* **2013**, *1*, 1002-1009.

[24] Utada, A. S.; Lorenceau, E.; Link, D. R.; Kaplan, P. D.; Stone, H. A.; Weitz, D. A. Monodisperse Double Emulsions Generated from a Microcapillary Device. *Science* **2005**, *308*, 537-541.

[25] Ekanem, E. E.; Zhang, Z.; Vladisavljevic, G. T. Facile microfluidic production of composite polymer core-shell microcapsules and crescent-shaped microparticles. *J. Colloid Interface Sci.* **2017**, *498*, 387-394.

[26] Kang, J. H.; Lee, S. S.; Guerrero, J.; Fernandez-Nieves, A.; Kim, S. H.; Reichmanis, E. Ultrathin Double-Shell Capsules for High Performance Photon Upconversion. *Adv. Mater.* **2017**, *29*, 1606830.

[27] Amato, D. V.; Lee, H.; Werner, J. G.; Weitz, D. A.; Patton, D. L. Functional Microcapsules via Thiol-Ene Photopolymerization in Droplet-Based Microfluidics. *ACS Appl. Mater. Interfaces* **2017**, *9*, 3288-3293.

[28] Hou, L.; Ren, Y.; Jia, Y.; Deng, X.; Tang, Z.; Tao, Y.; Jiang, H. A simple microfluidic method for one-step encapsulation of reagents with varying concentrations in double emulsion drops for nanoliter-scale reactions and analyses. *Anal. Methods* **2017**, *9*, 2511-2516.

[29] Kim, S. H.; Park, J. G.; Choi, T. M.; Manoharan, V. N.; Weitz, D. A. Osmotic-pressure-controlled concentration of colloidal particles in thin-shelled capsules. *Nat. Commun.* **2014**, *5*, 3068.

[30] Loiseau, E.; de Boiry, Q.; Niedermair, F.; Albrecht, G.; Ruhs, P. A.; Studart, A. R. Explosive Raspberries: Controlled Magnetically Triggered Bursting of Microcapsules. *Adv. Funct. Mater.* **2016**, *26*, 4007-4015.

[31] Thiele, J.; Chokkalingam, V.; Ma, S.; Wilson, D. A.; Huck, W. T. S. Vesicle budding from polymersomes templated by microfluidically prepared double emulsions. *Mater. Horiz.* **2014**, *1*, 96-101.

[32] Grolman, J. M.; Inci, B.; Moore, J. S. pH-Dependent Switchable Permeability from Core-Shell Microcapsules. *ACS Macro Lett.* **2015**, *4*, 441-445.

[33] Moore, D. G.; Brignoli, J. V. A.; Ruhs, P. A.; Studart, A. R. Functional Microcapsules with Hybrid Shells Made via Sol-Gel Reaction within Double Emulsions. *Langmuir* **2017**, *33*, 9007-9017.

[34] Guerzoni, L. P. B.; Bohl, J.; Jans, A.; Rose, J. C.; Koehler, J.; Kuehne, A. J. C.; De Laporte, L. Microfluidic fabrication of polyethylene glycol microgel capsules with tailored properties for the delivery of biomolecules. *Biomater. Sci.* **2017**, *5*, 1549-1557.

[35] Sakai, T.; Matsunaga, T.; Yamamoto, Y.; Ito, C.; Yoshida, R.; Suzuki, S.; Sasaki, N.; Shibayama, M.; Chung, U. Design and Fabrication of a High-Strength Hydrogel with Ideally Homogeneous Network Structure from Tetrahedron-like Macromolecules. *Macromolecules* **2008**, *41*, 5379-5384.

[36] Li, X.; Tsutsui, Y.; Matsunaga, T.; Shiayama, M.; Chung, U.; Sakai, T. Precise Control and Prediction of Hydrogel Degradation Behavior. *Macromolecules* **2011**, *44*, 3567-3571.

[37] Hayashi, K.; Okamoto, F.; Hoshi, S.; Katashima, T.; Zujur, D. C.; Li, X.; Shibayama, M.; Gilbert, E. P.; Chung, U.; Ohba, S.; Oshika, T.; Sakai, T. Fast-forming hydrogel with ultralow polymeric content as an artificial vitreous body. *Nat. Biomed. Eng.* **2017**, *1*, 0044.

[38] Long, M. S.; Cans, A. S.; Keating, C. D. Budding and Asymmetric Protein Microcompartmentation in Giant Vesicles Containing Two Aqueous Phases. *J. Am. Chem. Soc.* **2008**, *130*, 756-762.

[39] Shimanovich, U.; Song, Y.; Brujic, J.; Shum, H. C.; Knowles, T. P. J. Multiphase Protein Microgels. *Macromol. Biosci.* **2015**, *15*, 501-508.

[40] Vijayakumar, K.; Gulati, S.; deMello, A. J.; Edel, J. B. Rapid cell extraction in aqueous two-phase microdroplet systems. *Chem Sci.* **2010**, *1*, 447-452.

[41] Yasukawa, M.; Kamio, E.; Ono, T. Monodisperse water-in-water-in-oil emulsion droplets. *ChemPhysChem* **2011**, *12*, 263-266.

[42] Yuan, H.; Ma, Q.; Song, Y.; Tang, M. Y. H.; Chan, Y. K.; Shum, H. C. Phase-Separation-Induced Formation of Janus Droplets Based on Aqueous Two-Phase Systems. *Macromol. Chem. Phys.* **2017**, *218*, 1600422.

[43] Ma, S.; Thiele, J.; Liu, X.; Bai, Y.; Bell, C.; Huck, W. T. S. Fabrication of Microgel Particles with Complex Shape via Selective Polymerization of Aqueous Two-Phase Systems. *Small* **2012**, *8*, 2356-2360.

[44] Hann, S. D.; Lee, D.; Stebe, K. J. Tuning interfacial complexation in aqueous two phase systems with polyelectrolytes and nanoparticles for compound all water emulsion bodies (AWE-somes). *Phys. Chem. Chem. Phys.* **2017**, *19*, 23825-23831.

[45] Millqvist-Fureby, A.; Malmsten, M.; Bergenstahl, B. An Aqueous Polymer Two-Phase System as Carrier in the Spray-Drying of biological Material. *J. Colloid Interface Sci.* **2000**, *225*, 54-61.

[46] Atefi, E.; Lemmo, S.; Fyffe, D.; Luker, G. D.; Tavana, H. High Throughput, Polymeric Aqueous Two-Phase Printing of Tumor Spheroids. *Adv. Funct. Mater.* **2014**, *24*, 6509-6515.

[47] Torza, S.; Mason, S. G. Coalescence of Two Immiscible Liquid Drops. *Science* **1969**, *163*, 813-814.

[48] Byun, C. K.; Kim, M.; Kim, D. Modulating the Partitioning of Microparticles in Polyethylene Glycol (PEG)-Dextran (DEX) Aqueous Biphasic System by Surface Modification. *Coatings* **2018**, *8*, 85.

[49] Choi, S. -W.; Cheong, I. W.; Kim, J. -H.; Xia, Y. Preparation of Uniform Microspheres Using a Simple Fluidic Device and Their Crystallization into Close-Packed Lattices. *Small* **2009**, *5*, 454-459.

[50] Mytnyk, S.; Ziemecka, I.; Olive, A. G. L.; van der Meer, J. W. M.; Totlani, K. A.; Oldenhof, S.; Kreutzer, M. T.; van Steijn, V.; van Esch, J. H. Microcapsules with a permeable hydrogel shell and an aqueous core continuously produced in a 3D microdevice by all-aqueous microfluidics. *RSC Adv.* **2017**, *7*, 11331-11337.

[51] Aimar, P.; Meireles, M.; Sanchez, V. A. Contribution to the translation of retention curves into pore size distributions for sieving membranes. *J. Membrane Sci.* **1990**, *54*, 321-338.

[52] Matsunaga, T.; Sakai, T.; Akagi, Y.; Chung, U.; Shibayama, M. SANS and SLS Studies on Tetra-Arm PEG Gels in As-Prepared and Swollen States. *Macromolecules* **2009**, *42*, 6245-6252.
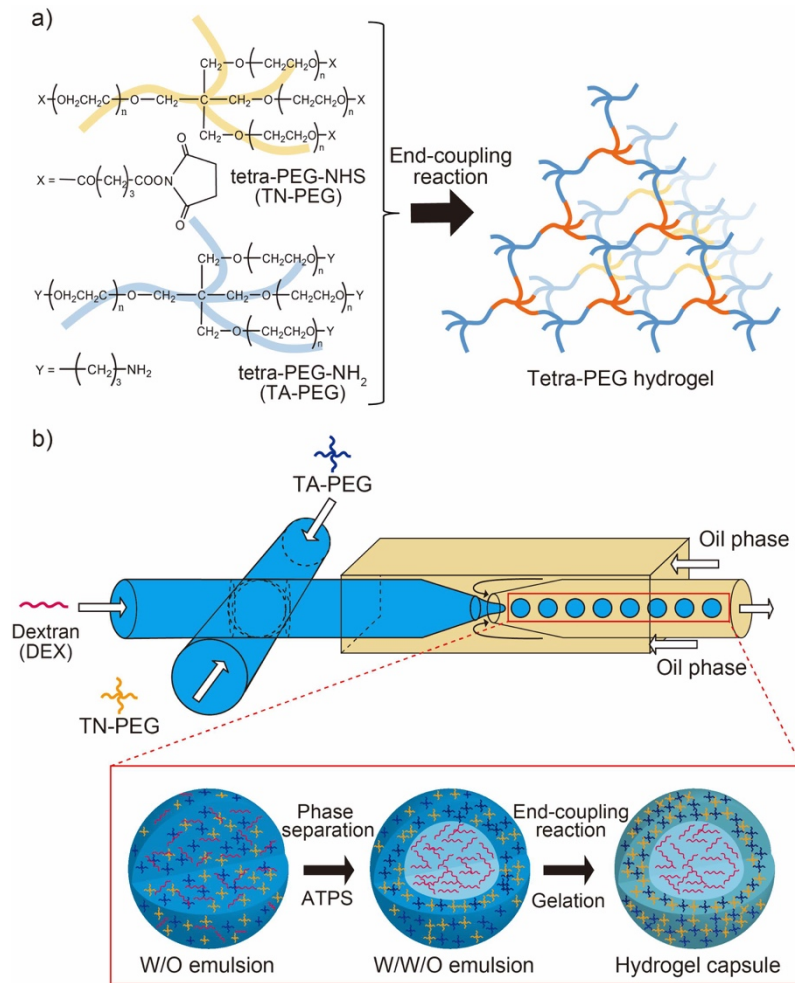
Figure 1 (a) Schematic image of the cross-end coupling reaction between tetra-PEG-NHS (TN-PEG) and tetra-PEG-NH$_2$ (TA-PEG) to synthesize tetra-PEG hydrogel. (b) Fabrication of tetra-PEG hydrogel microcapsules by combining microfluidic emulsification and phase separation within droplets, followed by cross-end coupling reaction in the shell.
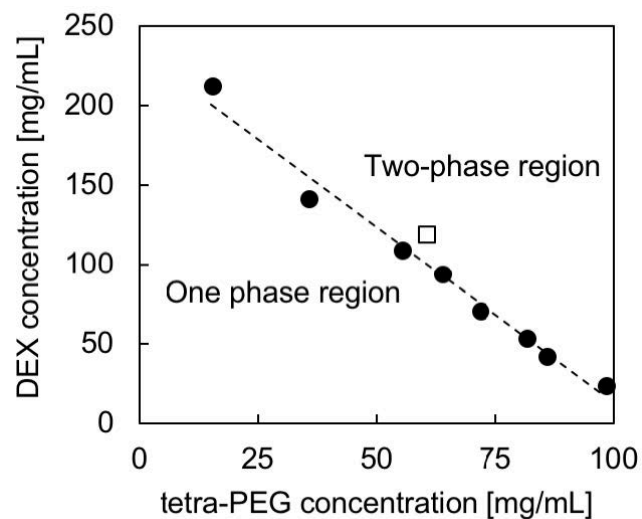
Figure 2 Phase diagram of TA-PEG/DEX system. The phase diagram shows the number of phases at different concentrations of TA-PEG (M_n = 10 kDa) and DEX (M_n = 40 kDa) in PBS (pH = 7.4) at 25°C. The dashed line indicates a binodal line that distinguishes one phase region from two-phase region. The open square symbol shows a standard ATPS composition used in this study.
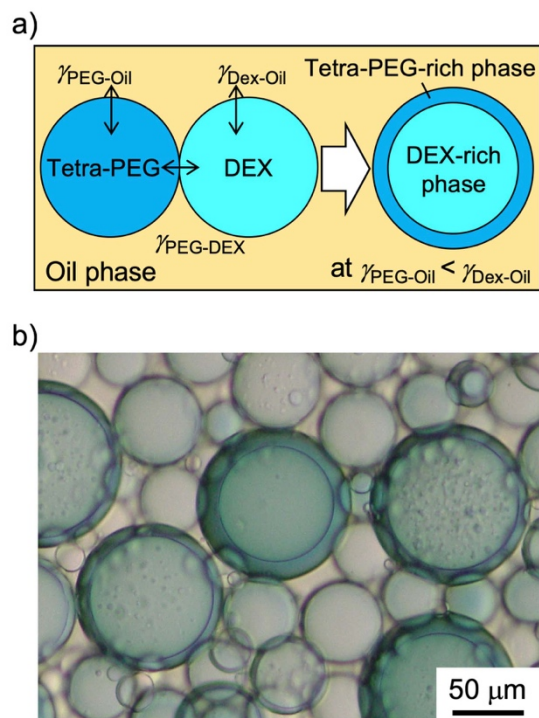
Figure 3 Formation of ATPS droplets based on internal phase separation. (a) Schematic image of ATPS droplets with a core-shell structure. (b) Optical microscopy image of polydisperse ATPS droplets dispersed in a tridecane solution containing 3 wt% Solsperse 19000 at 25°C. The concentrations of TA-PEG and DEX in the ATPS droplets were fixed at 60 mg/mL and 120 mg/mL, respectively.

Table 1 Interfacial tensions measured by the Wilhelmy plate method[1] (25°C).

Oil phase composition	$\gamma_{\text{Dex-Oil}}$ [mN/m]	$\gamma_{\text{PEG-Oil}}$ [mN/m]
3wt% Solsperse 19000 in tridecane	6.6	1.5
3wt% Span 80 in tridecane	2.5	< 1.0[2]
3wt% Solsperse 19000 in decane	2.3	< 1.0[2]
3wt% Span 80 in decane	2.9	< 1.0[2]
3wt% Solsperse 19000 in mineral oil	11.3	2.0
3wt% Span 80 in mineral oil	2.4	1.3
Tridecane w/o surfactant	37.1	18.2

[1] Concentrations of TA-PEG and DEX in each aqueous solution were fixed at 60 mg/mL and 120 mg/mL, respectively. [2] Interfacial tension was lower than the detection limit of the instrument.
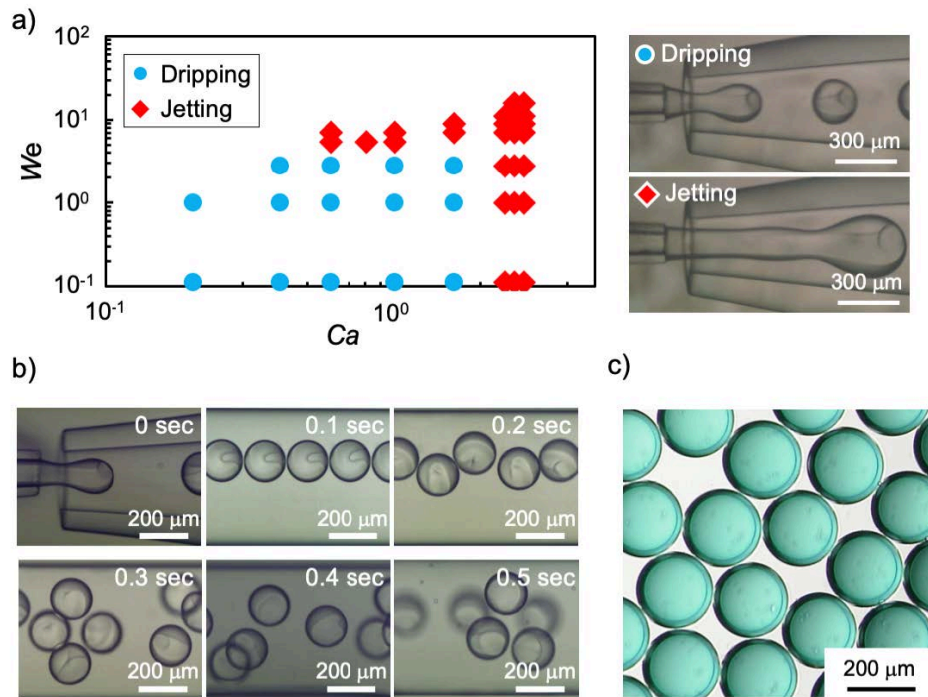
Figure 4 Formation of monodisperse ATPS droplets using a microfluidic device. (a)State diagram of the dripping to jetting transition on the capillary number of the outer flow and the Weber number of the inner flow of a capillary microfluidic device. Blue circle symbols represent dripping while red diamond symbols represent jetting. The concentrations of TA-PEG and DEX in the dispersed aqueous phase were fixed at 60 mg/mL and 120 mg/mL, respectively. The Q_d was described by the following equations: $Q_d = Q_{dTA-PEG} + Q_{dDEX}$, and $Q_{dTA-PEG} = 2Q_{dDEX}$. The continuous oil phase was a tridecane solution containing 3 wt% Solsperse 19000. (b) Time course of phase separation within monodisperse ATPS droplets travelling to the downstream of the microchannel (at Q_d = 150 μL/min and Q_c = 800 μL/min). (c) Optical microscopy image of monodisperse ATPS droplets dispersed in a tridecane solution containing 3 wt% Solsperse 19000. The flow rates of Q_d and Q_c were 90, 1,000 μL/min, respectively. The tetra-PEG macromonomer-rich phase was stained with Reactive Blue 160.
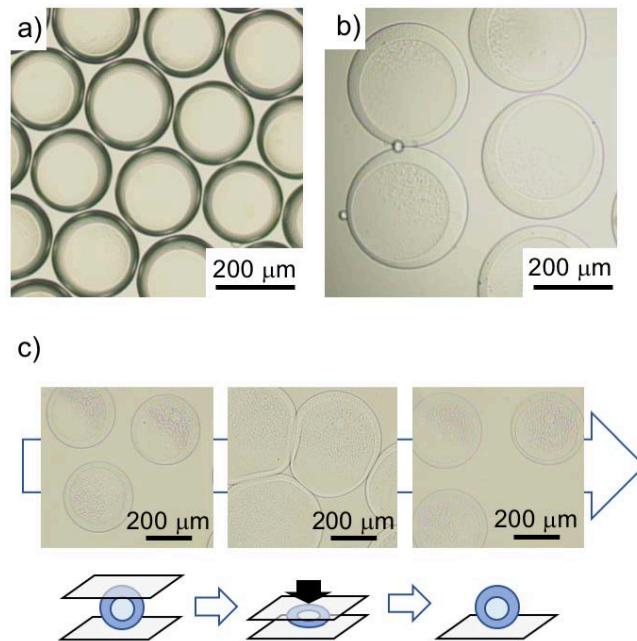
Figure 5 Optical microscopy images of tetra-PEG hydrogel microcapsules dispersed in (a) tridecane and (b) water. (c) Optical microscopy images of the hydrogel microcapsules during compression test. The hydrogel microcapsules were prepared at Q_d = 150 µL/min and Q_c =800 µL/min.
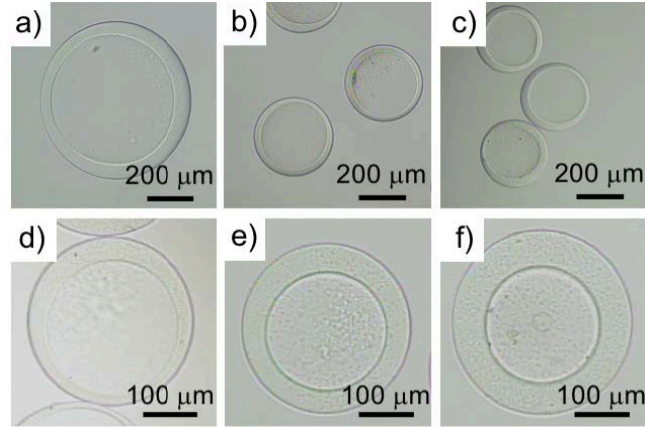
Figure 6 (a-c) Optical microscopy images of tetra-PEG hydrogel microcapsules with different diameters. Microcapsules with different diameters were prepared by varying the flow rates of Q_c at fixed Q_d (150 µL/min). The Q_c was (a) 300, (b) 500, and (c) 800 µL/min. (d-f) Optical microscopy images of tetra-PEG microcapsules with different shell thickness. Microcapsules having different shell thickness were prepared by varying the concentration ratio between DEX (C_{DEX}) and tetra-PEG macromonomers (C_{PEG}) in the dispersed phase. The C_{DEX}/C_{PEG} = (d) 2/1 (w/w) at Q_{dPEG} /Q_{dDEX} /Q_c = 100/50/800 µL/min (e) 1/1 (w/w) at Q_{dPEG} /Q_{dDEX} /Q_c = 100/25/800 µL/min, and (f) 1/2 (w/w) at Q_{dPEG} /Q_{dDEX} /Q_c = 100/12.5/800 µL/min).

Table 2 Effect of Q_c on the microcapsule size and inner core size, and the shell thickness to radius ratio.

| Q_c [µL/min]	300	500	800
Overall diameter [µm] (CV)	665.2 (6.7%)	343.5 (5.3%)	291.3 (2.6%)
Core diameter [µm]	539.1 (3.9%)	282.6 (4.0%)	243.5 (4.0%)
Shell thickness to Radius ratio (T/R (-))	0.19	0.18	0.16

Table 3 Effect of C_{DEX} / $C_{tetra\text{-}PEG}$ in the dispersed phase on the microcapsule size and inner core size, and the shell thickness to radius ratio.

| C_{DEX} / $C_{tetra\text{-}PEG}$ (w/w)	2/1	1/1	1/2
Overall diameter [μm] (CV)	311.5 (6.7%)	312.7 (5.3%)	315.0 (2.6%)
Core diameter [μm]	251.4 (8.7%)	224.0 (5.4%)	194.9 (4.3%)
Shell thickness to Radius ratio (T/R (-))	0.19	0.28	0.38
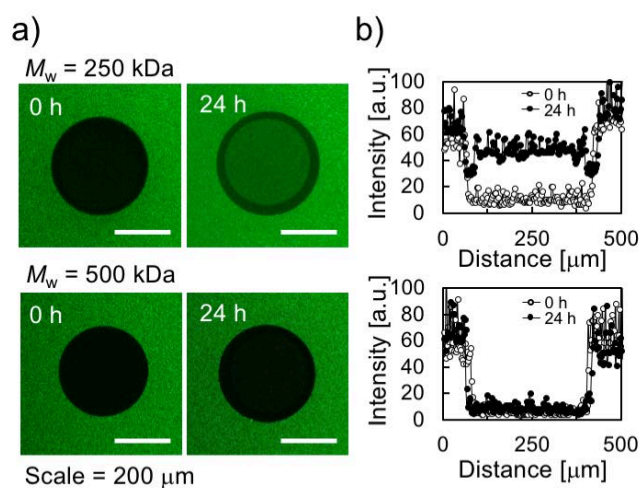
Figure 7 Permeability measurement of tetra-PEG hydrogel microcapsules. (a) Fluorescent images show the permeability of tetra-PEG hydrogel microcapsules to FITC-DEX with different molecular weights (M_w = 250 k and 500 kDa). (b) Fluorescent intensity profiles calculated from the images.
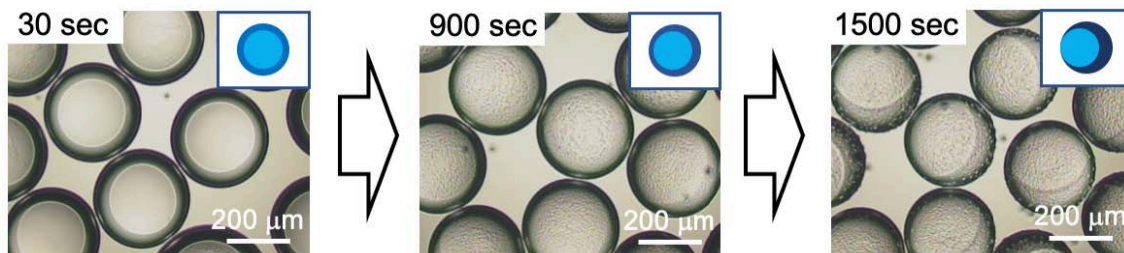
Figure 8 Optical microscopy images showing the time course of DEX/tetra-PEG Janus microparticles formation from W/W/O emulsion droplets during cross-end coupling reaction at pH 4.0. The inset images show the schematic images of ATPS droplets.
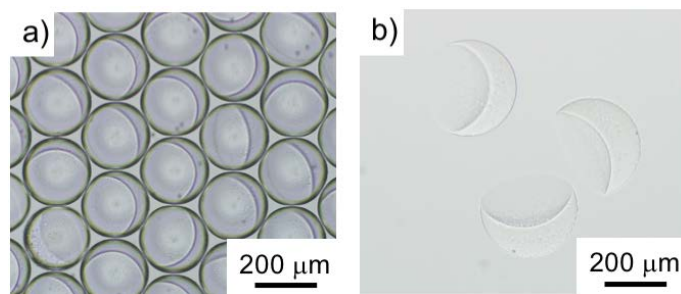
Figure 9 Optical microscopy images of tetra-PEG microparticles prepared at pH 4.0. The microcapsules were dispersed in (a) tridecane and (b) water. The C_{DEX}/C_{PEG} was 2/1 (w/w) at $Q_{dPEG}/Q_{dDEX}/Q_c = 100/50/800$ µL/min.
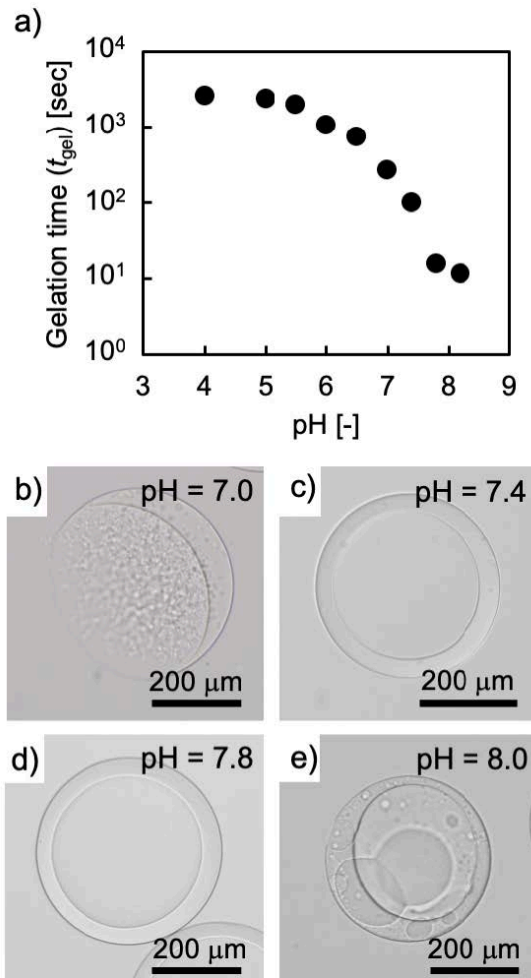
Figure 10 (a) Effect of pH on the gelation time (t_{gel}) of tetra-PEG hydrogel. (b-f) Representative optical microscopy images of tetra-PEG microparticles prepared at different pH conditions. The pH value and t_{gel} were (b) 7.0 [t_{gel} = 270 sec], (c) 7.4 [t_{gel} = 100 sec], (d) 7.8 [t_{gel} = 15 sec], and (e) 8.0 [t_{gel} = 13 sec]. The C_{DEX}/C_{PEG} was 2/1 (w/w) at $Q_{dPEG}/Q_{dDEX}/Q_c$ = 100/50/800 μL/min.

Graphical Abstract